

# Dynamic Interreceptor Coupling: A Novel Working Mechanism of Two-Dimensional Ryanodine Receptor Array

Xin Liang,\* Xiao-Fang Hu,\* and Jun Hu\*†

\*Bio-X Life Science Research Center, College of Life Science and Biotechnology, Shanghai Jiao Tong University, Shanghai, China; and †Shanghai Institute of Applied Physics, Chinese Academy of Sciences, Shanghai, China

**ABSTRACT** Ryanodine receptors (RyRs) usually form two-dimensional regular array in sarcoplasmic reticulum membranes in muscle cells. The inter-RyRs coupling may be essential for the maintenance of quiescent  $\text{Ca}^{2+}$  release in resting state, as well as for the coordinated activation and rapid termination of RyR-mediated  $\text{Ca}^{2+}$  release during excitation-contraction coupling. In our previous work, we have reported that the inter-RyRs interaction is modulated by RyR channel's functional state, which inspired us to propose a novel working mechanism of RyR array: "dynamic inter-RyR coupling". In this work, we built a simple model based on cellular automata and the Monte-Carlo method to quantitatively investigate the roles of intermolecular coupling and its modulation in regulating the signaling capabilities of RyR array. Our simulation results showed that with a suitable inter-RyR coupling strength, the combination of rest stability and high response efficiency, namely optimal signal/noise ratio, of  $\text{Ca}^{2+}$  signaling could be achieved. Moreover, we also found the continued coupling between open RyRs would delay the system termination rate. The coacquisition of robust termination of array opening relied on the proper decrease of coupling strength between activated RyRs. Obviously, such temporally asymmetric coupling would simultaneously endow the system with physiologically relevant resting stability and fast termination.

## INTRODUCTION

Ryanodine receptor (RyR) is the ion channel mediating  $\text{Ca}^{2+}$  release from endoplasmic/sarcoplasmic reticulum (SR) and plays a pivotal role in intracellular  $\text{Ca}^{2+}$  signaling processes, such as excitation-contraction coupling (E-C coupling), in all muscle cell types (1–4). It is long recognized that a large amount of  $\text{Ca}^{2+}$  is released from RyRs during E-C coupling by self-amplified calcium-induced calcium release (CICR) (5–7). But such positive feedback is unstable, it potentially undermines the resting stability of RyRs by amplifying noise  $\text{Ca}^{2+}$ , and it also potentially hinders the rapid termination of E-C coupling by regenerating  $\text{Ca}^{2+}$  release (5,6). Therefore, some design principles must be developed during evolution for RyRs to solve these problems.

Recently, electronic microscopy studies reveal that RyRs in either skeletal or cardiac muscle cells are almost exclusively found to be assembled into two-dimensional paracrystalline arrays in SR membrane (8–10). This organization pattern is highly conserved from crustaceans to vertebrates, suggesting that the array formation is critical to RyR-mediated  $\text{Ca}^{2+}$  release in muscle physiology (8,10,11). Some mechanism based on the RyR array may be developed to solve the problems accompanying CICR. Based on the observation of coordinated gating of neighboring RyRs in in vitro electrophysiological experiments (12–14), it has been proposed

by Stern et al. that the allosteric interaction between neighboring resting RyRs in the array would stabilize RyRs in closed state, thus the inter-RyRs coupling provides a mechanism for the resting stability (6). However, the constant RyR-RyR coupling brings a potential design paradox into the termination process of RyR-mediated  $\text{Ca}^{2+}$  release in E-C coupling (5,15). It should be noted that in the presence of self-regenerative CICR, the rapid closure of the activated RyR channel array largely relies on the efficiency of negative feedback. Just as coupling does for resting RyRs, the continued coupling between activated RyRs will result in the stabilization of RyRs in their open state. Under such design constraints, termination mechanisms cannot efficiently transfer RyRs from open state to closed state (5,12,15). With the prolonged opening duration, both the global and local stability of SR  $\text{Ca}^{2+}$  signaling would be lost (6,16).

Intuitively, this design paradox can be ameliorated by introducing different coupling states between closed RyRs and between open RyRs. While strong coupling between closed RyRs is required to ensure the resting stability, a decoupling of RyRs accompanying their activation may remove the negative effect of inter-RyRs coupling on the termination process. This mechanism is recently hinted by our in vitro observations that the interaction between isolated RyRs decreases when the channels are activated (17). Moreover, the latest study on coupled gating of RyRs by Dulhunty et al. also reported that synchronized opening of three coupled RyRs is followed by multiple transitions between 1, 2, or 3 channels (18), which also suggested the loose coupling between activated RyRs in closing reaction. Obviously, such dynamic coupling would have profound impacts on the RyR array operation and function.

Submitted June 7, 2006, and accepted for publication October 20, 2006.

Address reprint requests to Dr. Xiao-Fang Hu, Bio-X Life Science Research Center, College of Life Science and Biotechnology, Shanghai Jiao Tong University, Shanghai, China. Tel: 86-21-34204875; Fax: 86-21-34204872; E-mail: xfhu@sjtu.edu.cn.

**Abbreviations used:** RyR, ryanodine receptor/calcium release channel; SR, sarcoplasmic reticulum; E-C coupling, excitation-contraction coupling; DHP, dihydropyridine receptor; SNR, signal/noise ratio.

© 2007 by the Biophysical Society

0006-3495/07/02/1215/09 \$2.00

doi: 10.1529/biophysj.106.090670

In this work, we applied a typical SR  $\text{Ca}^{2+}$  release model to quantitatively examine the impact of such dynamic coupling of RyRs on the resting stability and  $\text{Ca}^{2+}$  release duration of the two-dimensional (2-D) channel array. We demonstrated that the strong coupling between resting RyRs could increase the stability of array under rest, and an optimal coupling strength could be found for RyR array to achieve the combination of the low noise and high response efficiency, namely optimal signal/noise ratio (SNR). Moreover, the coacquisition of the timely closure of the array relied on a proper decrease of the coupling strength between activated RyRs. Our results clearly showed that such state-dependent coupling between neighboring receptors would provide a simple and efficient way to improve signaling performance of the system. In addition, the normal operation of RyR array under SR  $\text{Ca}^{2+}$  release could be dramatically damaged by biased regulation of inter-RyRs coupling, for instance in some pathological states, which would also be discussed in this paper.

## MODEL LAYOUT

### Gating scheme of single ryanodine receptor

We considered both activation and inactivation of  $\text{Ca}^{2+}$  on the activity of RyRs (2,4). Then given the law of conservation of mass and energy, a four-state scheme was built to describe RyR gating (Fig. 1 B), in which there are three closed states ( $C_1, C_2, C_3$ ) and one open state (O). The transition probability of RyRs between different states was determined by the kinetic parameters in Table 1. The values of these parameters were set mainly according to current knowledge of single RyR gating (4), but because the RyR gating

scheme in vivo is not very clear now, two additional points need to be particularly described:

1. It is still not very clear how many  $\text{Ca}^{2+}$  ions could activate the RyR in CICR (5). In our model,  $\text{Ca}^{2+}$  activation was set to be dependent on the second power of the  $\text{Ca}^{2+}$ , in an effort to be consistent with data demonstrating that the rate of  $\text{Ca}^{2+}$  sparks is dependent on the square of  $[\text{Ca}^{2+}]_i$  (5).
2. The inherent mechanism by which clustered RyRs are closed during SR calcium release is a fundamental question not yet answered (15). In our model, accelerated  $\text{Ca}^{2+}$ -dependent inactivation (with  $K_d \approx 10 \mu\text{M}$ ; see Table 1) (6) was used as negative feedback mechanism in the gating scheme of single RyR, which is mainly based on the following considerations: 1), Some inactivation mechanisms do exist in SR  $\text{Ca}^{2+}$  signaling, in the absence of which  $\text{Ca}^{2+}$  release could not be terminated timely (4,15,19). 2), Although the  $\text{Ca}^{2+}$ -dependent inactivation observed in in vitro single channel recordings (with  $K_d \approx 1 \text{ mM}$ ) (4) is too slow to close the RyR array in vivo, the feasibility of accelerated in vivo  $\text{Ca}^{2+}$  inactivation was already proposed to be coupled to the activity of  $\text{Ca}^{2+}$ -dependent molecules, e.g., calmodulin (CaM) (20). Because it is widely accepted that the gating scheme of RyRs should be reshaped by numerous in vivo factors, we think this modification for the modeling requirement should be acceptable.

### Two-dimensional tetragonal lattice model of RyRs

Electronic microscope studies revealed that the geometry of the lattice and the number of RyRs in the lattice (usually

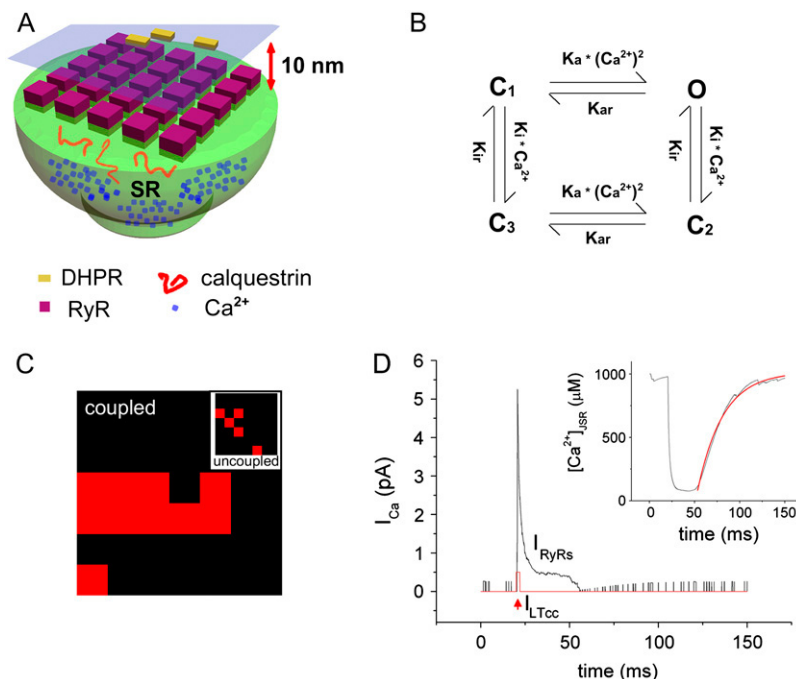


FIGURE 1 Modeling layout and basic simulations. (A) Three-dimensional spatial layout of model elements. (B) Four-state gating scheme of a single ryanodine receptor (RyR) with three closed states and one open state. (C) Instantaneous pictures of coupled ( $e = 0.25$ ,  $\alpha = 1.0$ ) and uncoupled RyR array (inset,  $e = 0$ ,  $\alpha = 1.0$ ). (D) Basic simulations of our model ( $e = 0.4$ ,  $\alpha = 1.0$ ): curves of SR  $\text{Ca}^{2+}$  current and  $\text{Ca}^{2+}$  content in JSR (inset) during once array opening. The red pulse curve represented the triggering  $\text{Ca}^{2+}$  signal from one L-type  $\text{Ca}^{2+}$  channel (LTCC), and three LTCCs were included in the simulations with 25 RyRs. The recovery  $\text{Ca}^{2+}$  current in JSR could be well fitted to the first-order exponential curve with the time constant of  $\sim 30 \text{ ms}$ .

**TABLE 1** Kinetic constants of RyRs' gating scheme

Name	Meaning	Value
$K_a$	On-rate of $\text{Ca}^{2+}$ activation	$10.0 (\mu\text{M}^{-2} \times \text{s}^{-1})$
$K_i$	On-rate of $\text{Ca}^{2+}$ inactivation	$2 (\mu\text{M}^{-1} \times \text{s}^{-1})$
$K_{ar}$	Off-rate of $\text{Ca}^{2+}$ activation	$400.0 (\text{s}^{-1})$
$K_{ir}$	Off-rate of $\text{Ca}^{2+}$ inactivation	$20 (\text{s}^{-1})$

10~100) varies with the species and muscle types (8). In this model, the typical square lattice formed of 25 ( $5 \times 5$ ) receptors (Fig. 1 C) was adopted. Here, it should be pointed out that we also run the simulations with RyR arrays in various sizes, and the main conclusions of our manuscript are not affected by the size of RyR array. We consulted the arithmetic proposed by Stern et al. (6), by which the intermolecular coupling was introduced into the kinetics of arrayed RyRs (Eq. 1):

$$K_{ij} = k_{ij} \times e^{\sum_{m=1}^n (E_{jsm} - E_{ism}) / (kT)}, \quad (1)$$

where  $K_{ij}$  is the kinetic parameter of coupled RyRs;  $k_{ij}$  is the kinetic parameter of isolated RyRs;  $E_{ij}$  is the interaction energy between two contacting RyRs;  $i/j$  is current/next state of central RyR;  $s_m$  is the state of neighboring RyR;  $n$  represented the number of physical contacting neighbors of the central RyR.

Here, to present a more intuitive impression of the operation of the RyR array in our model, instantaneous cartoon pictures of uncoupled and coupled RyRs array were captured during array operation. In an uncoupled system, RyRs opened individually (*inset* of Fig. 1 C). Small patches of open channels stochastically appeared, but rarely. However, in a coupled system, opening events could be found in large patches of activated RyRs (Fig. 1 C). Furthermore, a coefficient matrix was constructed to modify the interaction energy ( $e$ ) between neighboring RyRs in state-dependent manner (Eq. 2). The standard principles to evaluate the coefficients, “1” and “ $\alpha$ ”, in the matrix were described as following:

$$E_{ij}/kT = \begin{pmatrix} & C_1 & O & C_2 & C_3 \\ C_1 & 1 & -1 & -1 & -1 \\ O & -1 & \alpha & -\alpha & -1 \\ C_2 & -1 & -\alpha & \alpha & -1 \\ C_3 & -1 & -1 & -1 & 1 \end{pmatrix} \times e. \quad (2)$$

**Principle 1.** To realize intermolecular cooperativity, the neighbors in the same state with central receptor stabilize the central one, while the neighbors in alternative states impel the central one away from its current state. Given the form of Eq. 1, the interaction energy between contacting RyRs in the same/different states should be positive/negative, respectively.

**Principle 2.** We have reported that the interaction between RyRs would decrease when RyRs were activated by

$\text{Ca}^{2+}$ . To briefly but reasonably introduce this new information, we assumed that when two neighboring RyRs both bound to the activating  $\text{Ca}^{2+}$ , the interaction strength between them would change. In the above matrix, “ $\alpha$ ” is the coefficient for the interaction energy between two RyRs bound to activating  $\text{Ca}^{2+}$  (states O or  $C_2$ ). This parameter could be adjusted to simulate state-dependent coupling of arrayed RyRs in our model.

### In situ SR calcium release model

The in situ SR calcium release model adopted here was modified from Sobie's model for  $\text{Ca}^{2+}$  sparks (16), and the following described the model details. Fig. 1 A showed the spatial configuration of the SR  $\text{Ca}^{2+}$  release unit. It consisted of several different spatial regions, including the T-Tubule membrane (TTM) with L-type  $\text{Ca}^{2+}$  channels (LTCCs), SR membrane (SRM) with a regular array of RyRs, the nano-scale space between sarcolemma (SL) and SRM subspace, the cytoplasm, the space in junctional SR (JSR), and the extensive space of network SR (NSR).

First, the volume of subspace ( $V_{ss}$ ) was calculated as follows with the shape of the subspace simplified to be a column, and the RyR array, a regular square:

$$V_{ss} = D_{ss} \times \pi \times \left( \frac{1}{2} \times 30 \text{ nm} \times \sqrt{n_{\text{RyR}}} \times \sqrt{2} \right)^2, \quad (3)$$

where  $D_{ss}$  was the distance between SRM and TTM,  $\sim 10$  nm; 30 nm was the dimension of a RyR (9);  $n_{\text{RyR}}$  was the number of RyRs in the square array.

The concentration of  $\text{Ca}^{2+}$  in the subspace was determined by the  $\text{Ca}^{2+}$  influx through LTCCs ( $J_{\text{LTCCs}}$ ) and RyRs ( $J_{\text{RyRs}}$ ), the contribution of several  $\text{Ca}^{2+}$  buffers ( $J_{\text{buf}}$ ) and the  $\text{Ca}^{2+}$  efflux ( $J_{\text{efflux}}$ ) to the cytoplasm through diffusion:

$$\frac{d[\text{Ca}^{2+}]_{ss}}{dt} = J_{\text{LTCCs}} + J_{\text{RyRs}} + J_{\text{efflux}} + J_{\text{buf}}. \quad (4)$$

The startup of RyR array opening was normally stimulated by the inward  $\text{Ca}^{2+}$  current through the LTCCs in the TTM, and the number of LTCCs was determined according to the 7.3 RyRs/LTCCs (25 RyRs / 3 LTCCs) reported earlier (21). To emphasize our main point, a highly simplified L-type  $\text{Ca}^{2+}$  current ( $I_{\text{LTCC}} = 0.5$  pA,  $t_{\text{duration}} = 2$  ms) was used to replace detailed gating behavior of LTCCs. In formula 3,  $I_{\text{LTCCs}}$  represented the average  $\text{Ca}^{2+}$  current of opening LTCCs,  $F$  is the Faraday's constant, and  $V_{ss}$  is the volume of subspace.

$$J_{\text{LTCCs}} = N_{\text{LTCCs}} \times J_{\text{LTCC}} \quad (5)$$

$$J_{\text{LTCC}} = -\frac{I_{\text{LTCC}}}{2 \times F \times V_{ss}}. \quad (6)$$

$\text{Ca}^{2+}$  flux through the RyR was proportional to the  $\text{Ca}^{2+}$  concentration gradient between two sides of the SRM, and also correlated to the  $\text{Ca}^{2+}$  diffusion through the channel ( $D_{\text{RyR}}$ ).

$$J_{\text{RyR}} = D_{\text{RyR}} \times ([\text{Ca}^{2+}]_{\text{lumen}} - [\text{Ca}^{2+}]_{\text{ss}}). \quad (7)$$

The total  $\text{Ca}^{2+}$  efflux ( $J_{\text{RyRs}}$ ) through all the RyRs in the array was described as

$$J_{\text{RyRs}} = N_{\text{RyRs}_{\text{open}}} \times J_{\text{RyR}}. \quad (8)$$

In the subspace,  $\text{Ca}^{2+}$  could bind to calmodulin (CaM) and  $\text{Ca}^{2+}$  buffers in SRM and SL, the equation for these reactions could be written in a general form as following:

$$(\text{Buffer})_{\text{free}} + \text{Ca}^{2+} \xrightleftharpoons[K_{\text{off}}]{K_{\text{on}}} (\text{Buffer} - \text{Ca}^{2+})_{\text{complex}}. \quad (9)$$

So, the contribution of total  $J_{\text{buf}}$  should be calculated as

$$J_{\text{buf}} = \sum_{i=\text{SRM}_{\text{buf}}, \text{SL}_{\text{buf}}, \text{CaM}} K_{\text{off}}^i \times ([\text{buffer}_i]_{\text{total}} - [\text{buffer}_i]_{\text{free}}) - K_{\text{on}}^i \times [\text{Ca}^{2+}]_{\text{ss}} \times [\text{buffer}_i]_{\text{free}}. \quad (10)$$

$\text{Ca}^{2+}$  efflux to global cytoplasm through diffusion was determined by the  $\text{Ca}^{2+}$  concentration gradient and the velocity of  $\text{Ca}^{2+}$  diffusion. The  $[\text{Ca}^{2+}]_{\text{cyo}}$  was fixed at 100 nM and the  $\tau_{\text{efflux}}$  was the time constant for  $\text{Ca}^{2+}$  diffusing from subspace to cytoplasm.

$$J_{\text{efflux}} = \frac{1}{\tau_{\text{efflux}}} \times ([\text{Ca}^{2+}]_{\text{cyo}} - [\text{Ca}^{2+}]_{\text{ss}}). \quad (11)$$

Similar with the situation in subspace, three factors were mainly responsible for the calcium kinetics in JSR: outward  $\text{Ca}^{2+}$  current through RyRs, calcium flux from extensive NSR to JSR and the calcium buffer (calsequestrin) in JSR. Here,  $[\text{Ca}^{2+}]_{\text{NSR}}$  was fixed at  $10^3 \mu\text{M}$  and  $\text{Ca}^{2+}$  buffering in JSR by calsequestrin was treated as a rapid buffering process. Notably, the value of  $\tau_{\text{refill}}$  was changed from 10 ms in Sobie's model to 4 ms here. We made this modification to satisfy the recovery time constant ( $\sim 30$  ms) of free  $[\text{Ca}^{2+}]$  in JSR (Fig. 1 D), which was reported by the latest work of Brochet et al. (19).

$$\frac{d[\text{Ca}^{2+}]_{\text{lumen}}}{dt} = \beta_{\text{JSR}} \times (-J_{\text{RyRs}} \times V_{\text{ss}}/V_{\text{JSR}} + J_{\text{refill}}) \quad (12)$$

$$J_{\text{refill}} = \frac{1}{\tau_{\text{refill}}} \times ([\text{Ca}^{2+}]_{\text{NSR}} - [\text{Ca}^{2+}]_{\text{lumen}}) \quad (13)$$

$$\beta_{\text{JSR}} = [1 + \frac{[\text{CSQ}]_{\text{tot}} \times K_{\text{CSQ}}}{(K_{\text{CSQ}} + [\text{Ca}^{2+}]_{\text{lumen}})^2}]^{-1}. \quad (14)$$

The definitions and value of all the coefficients in our model were presented in Table 2. The basic simulations of our model under typical condition ( $e = 0.4$ ,  $\alpha = 1.0$ ) is shown in Fig. 1 D. Note that the opening of RyR array could be induced by a brief inward  $\text{Ca}^{2+}$  current through L-type  $\text{Ca}^{2+}$  channels to produce a large SR  $\text{Ca}^{2+}$  release ( $\sim 5$ – $6$  pA), reflecting the high gain of this system (Fig. 1 D). And there was an obvious reduction of  $\text{Ca}^{2+}$  content in JSR (*inset* in Fig. 1 D). Obviously, the sample curves derived from our model exhibited similar shape and quantitative features of

**TABLE 2 SR  $\text{Ca}^{2+}$  release model parameters**

Name	Definition	Value
$N$	Number of RyRs in the array	25 ( $5 \times 5$ )
$D$	$\text{Ca}^{2+}$ diffusion coefficient through an open RyR	$4000 \text{ s}^{-1}$
$F$	Faraday's constant	$96,480 \text{ C mol}^{-1}$
$\tau_{\text{ss}}$	Time constant of $\text{Ca}^{2+}$ diffusion into cytoplasm	$0.7 \mu\text{s}$
$[\text{Ca}^{2+}]_{\text{L}}$	$\text{Ca}^{2+}$ concentration in JSR	(initial) $1.0 \text{ mM}$
$V_{\text{ss}}$	Volume of subspace	$0.35 \times 10^{-12} \mu\text{L}$
$\text{CaM}$	Total calmodulin	$24.0 \mu\text{M}$
$K_{\text{on}}, \text{CaM}$	CaM $\text{Ca}^{2+}$ on-rate constant	$100 \mu\text{M}^{-1} \text{ s}^{-1}$
$K_{\text{off}}, \text{CaM}$	CaM $\text{Ca}^{2+}$ off-rate constant	$38 \text{ s}^{-1}$
$\text{SR}$	Total SR buffer	$47.0 \mu\text{M}$
$K_{\text{on}}, \text{SR}$	SR buffer on-rate constant	$115.0 \mu\text{M}^{-1} \text{ s}^{-1}$
$K_{\text{off}}, \text{SR}$	SR buffer off-rate constant	$100 \text{ s}^{-1}$
$\text{SL}$	Total SL buffer	$1124.0 \mu\text{M}$
$K_{\text{on}}, \text{SL}$	SL buffer on-rate constant	$115.0 \mu\text{M}^{-1} \text{ s}^{-1}$
$K_{\text{off}}, \text{SL}$	SL buffer off-rate constant	$1000.0 \text{ s}^{-1}$
$V_{\text{JSR}}$	Volume of JSR	$1 \times 10^{-11} \mu\text{L}$
$\tau_{\text{tr}}$	Time constant of $\text{Ca}^{2+}$ refill from NSR	$4 \times 10^{-3} \text{ s}$
$[\text{Ca}^{2+}]_{\text{NSR}}$	$\text{Ca}^{2+}$ concentration in NSR	$1.0 \text{ mM}$
$[\text{CSQ}]_{\text{tot}}$	Total CSQ in JSR	$10 \text{ mM}$
$K_{\text{CSQ}}$	CSQ $\text{Ca}^{2+}$ dissociation constant	$0.8 \text{ mM}$
$[\text{Ca}^{2+}]_{\text{cyt}}$	$\text{Ca}^{2+}$ concentration in cytoplasm	$0.1 \mu\text{M}$

SR  $\text{Ca}^{2+}$  release events observed experimentally (3,16,22–24), thereby demonstrating the workability of our model.

## Parameters and calculation

### Signal/noise ratio

Signal/noise ratio (SNR) was defined as the ratio between a signal (effective output) and the background (noise). It has been used as an evolutionary standard to determine the optimal coupling strength between bacterial chemotactic receptors by Shimizu et al. (25). In our model, the array's response to background  $\text{Ca}^{2+}$  and L-type  $\text{Ca}^{2+}$  current were treated as noise and signal, respectively. The SNR was calculated as following (Eq. 15):

$$\begin{aligned} \text{Signal} &= \frac{1}{n} \times \sum_{i=1}^{n=100} I_{\text{RyRs}}^{\text{peak}}(i)_{\text{L}} \\ \text{Noise} &= \text{Average}(I_{\text{RyRs}})_{\text{rest}} \\ \text{SNR} &= \frac{\text{Signal}}{\text{Noise}}. \end{aligned} \quad (15)$$

Here, signal was represented as the average amplitude of array response to input L-type  $\text{Ca}^{2+}$  current, and noise was the average SR  $\text{Ca}^{2+}$  current from arrayed RyRs under resting state by continuously running the program for  $3 \times 10^7$  time steps (biological time = 3 s, much longer than the operation cycle of array opening).

### Computation

The operation of the RyR lattice array during SR calcium release was run based on cellular automata and the Monte-Carlo

method with the time step of  $10^{-7}$  s. All programs were allowed to run a period of time (usually  $2 \times 10^6$  time steps/biological time = 200 ms) for stabilization before the beginning of experimental simulations. And all the codes for this model were written in Fortran and operated on a Dell workstation for scientific computation.

## RESULTS AND DISCUSSION

### Resting stability and high response efficiency of coupled RyR array

The impact of inter-RyR coupling on the RyR array's resting stability and response efficiency to input triggering signal was quantitatively investigated.

For an uncoupled system, all the receptors in the array behaved individually. Though the open probability of solitary RyRs under steady state ( $0.1 \mu\text{M Ca}^{2+}$ ) is very low ( $P_o < 0.01$ ), the activation of the entire RyR array would be largely maintained due to the positive feedback of  $\text{Ca}^{2+}$ -mediated regeneration (Fig. 2 A (a)). Such frequent spontaneous activation of uncoupled RyR array greatly increased the resting noise of system. If we simulated the DHPR-generated  $\text{Ca}^{2+}$  current and input such triggering  $\text{Ca}^{2+}$  signals to the RyR array (arrows in Fig. 3 A (a)), it was found that this signal was submerged in a sea of  $\text{Ca}^{2+}$  noise, and the RyR array could not respond efficiently to the triggering signal (Fig. 3 A (a)). The questions arose that how could RyR array keep resting stability and response efficiency in vivo?

The functional cooperation between neighboring RyRs under resting conditions provides a possible way to solve the problems. Running simulations with different cooperativity between RyRs allowed us to investigate the detailed roles of coupling in array operation. When the RyR-RyR interaction energy ( $e$ ) was increased to 0.35 (Fig. 2 A (b)), the continued opening of system changed into individual opening events. If further increasing the interaction energy to 0.6 ( $e$ ) (Fig. 2 A

(c)), the system exhibited low level of noise. Statistically analysis showed that spontaneous  $\text{Ca}^{2+}$  current through RyR array decreased monotonically with the increase of inter-RyR interaction energy, and the array could keep quite stable when interaction energy ( $e$ ) was more than 0.4 (Fig. 2 B).

Correspondingly, we also examined the impact of coupling strength on the RyR array's response to triggering signal. Suitably strengthening the inter-RyR coupling ( $e = 0.35$ ) could efficiently stand out the response of RyR array to triggering  $\text{Ca}^{2+}$  signal (Fig. 3 A (b)). On the other hand, we also saw that too much strong interaction between RyR would make the array "blind" to the input signal (Fig. 3 A (c)). As shown in Fig. 3 B, the mean amplitude of system response showed biphasic dependence on coupling strength ( $e$ ). The  $e$ -dependent amplitude curve rose in the region of  $0 \sim 0.4$  ( $e$ ), but in the region of  $0.5 \sim 0.7$  ( $e$ ), the response amplitude decreased with the increase of interaction energy. The maximum response gain could be observed at  $0.4 \sim 0.5$  ( $e$ ).

Thus, the range of interaction energy suitable to maintain both RyR array resting stability and response efficiency is in the region of  $0.4 \sim 0.5$  ( $e$ ). In further searching for the optimal interaction energy, we determined the system SNR in response to a  $\text{Ca}^{2+}$  stimulus (mildly above activation threshold). The SNR showed bell-shaped interaction energy ( $e$ ) dependence, with the maximum SNR at  $0.45 \sim 0.6$  interaction energy (Fig. 3 B). Comprehensively considering the optimal SNR and high response efficiency of RyR array, it was expected that when coupling strength ( $e$ ) was in  $0.45 \sim 0.5$ , the resting stability and response efficiency of the system were best integrated.

### Effects of " $\alpha$ " on resting stability and response efficiency

All the results mentioned above were obtained for a RyR array with constant coupling strength ( $\alpha = 1.0$ ). To investigate the effect of the coupling strength between activated RyRs on the resting stability and response efficiency of RyR array, we ran the simulations with various " $\alpha$ ". As shown in Fig. 4, A and B, the decrease of  $\alpha$  from 1.0 to 0, with the interval of 0.2, had little effect on the  $e$ -dependent curves for both resting stability and response amplitude of RyR array. Obviously, the coupling strength between neighboring activated RyRs, represented as " $\alpha$ ", is relatively independent with the system behavior in resting state and activation stage.

Based on these results, we noted that two factors should be responsible for the resting stability and high response efficiency of RyR array. First is the coupling between two neighboring resting RyRs, and second is the inhibitory effect from resting RyRs to their opening neighbors. These two factors keep the RyR array stable enough under rest through increasing the activation threshold for RyR array. It should be noted that the high response efficiency depends on the resting stability. The maximum amplitude appeared only

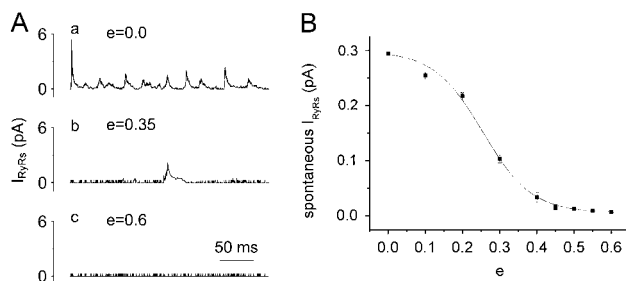


FIGURE 2 Effects of inter-RyR coupling strength on the resting stability of a RyR array. (A) The typical activity curves of RyR array with different coupling strength under rest: (a)  $e = 0$ ; (b)  $e = 0.35$ ; (c)  $e = 0.6$ . (B)  $E$ -dependent curve of spontaneous opening of RyR array, in which the data dots are the average results of 10 simulations for  $10^7$  time steps (biological time = 1 s). For clarity, all the results shown here are obtained when " $\alpha$ " was 1.0.

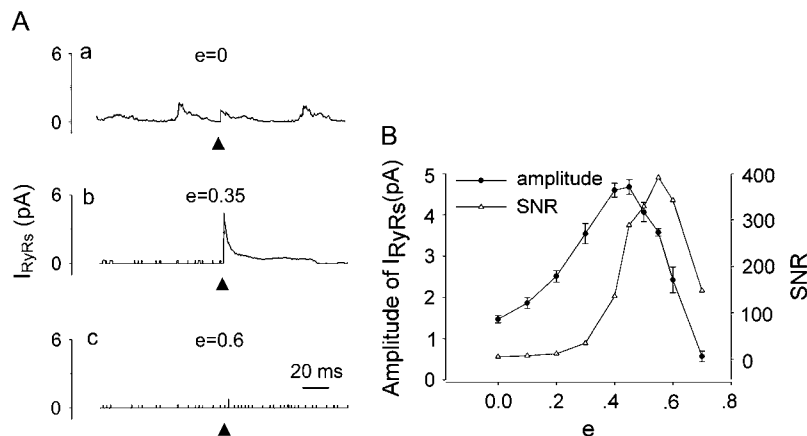


FIGURE 3 Effects of inter-RyR coupling strength on response amplitude and SNR of a RyR array. (A) The typical response of RyR array with different coupling strength to input  $Ca^{2+}$  signal: (a)  $e = 0$ ; (b)  $e = 0.35$ ; (c)  $e = 0.6$ . The arrows indicate the time of triggering L-type  $Ca^{2+}$  current. (B) Regulation of coupling energy ( $e$ ) on response efficiency and SNR of system. The data dots of amplitude curve are averaged from 100 simulations of SR  $Ca^{2+}$  release events, while SNR is calculated based on the formula described in the Model Layout section. For clarity, all the results shown here were obtained when “ $\alpha$ ” was 1.0.

when the coupling strength ( $e$ ) between RyRs is strong enough to stabilize the system under rest (Figs. 3 B and 4 B). Therefore, the coupling between resting RyRs and their (closed/opening) neighbors play pivotal roles in keeping the system stability and response efficiency, while the coupling between activated RyRs contributes little on the performance of RyR array in this stage.

### Effect of “ $\alpha$ ” on opening duration of RyR array

#### Coacquisition of rapid termination in a coupled system

From the evolutionary point of view, systems with both optimal SNR and high response efficiency should be favored (25) in cellular signaling. For an array of channels such as the RyR array in SR, rapid closure of the system is also physiologically required. Because the duration of array opening cannot be directly measured in vivo at present, what little knowledge we have of the process has been obtained from the analysis of temporal characteristics of elementary SR  $Ca^{2+}$  events, e.g.,  $Ca^{2+}$  sparks and  $Ca^{2+}$  blinks. First, Soeller and Cannell reconstructed the SR  $Ca^{2+}$  flux underlying  $Ca^{2+}$  sparks peaked in  $\sim 5$  ms and decayed with halftime of  $\sim 5$  ms (22), which suggested that total duration of RyR array should be longer than 10 ms. More recently, Brochet et al. reported the time to nadir of  $Ca^{2+}$  blinks was  $\sim 22$  ms, longer than the time to peak of  $Ca^{2+}$  sparks (in rat ventricular myocytes  $\sim 10$  ms) (19). In principle, the  $Ca^{2+}$  in JSR would not decrease

further after the complete closure of RyRs, therefore the temporal characteristics of  $Ca^{2+}$  blinks suggested that the opening of clustered RyRs should be at least 22 ms. Therefore, 22 ms might be the proximal value that reflected the actual duration of clustered RyRs underlying the  $Ca^{2+}$  sparks at the present.

To favor the optimal SNR of system, the interaction energy was selected to be 0.45. We first tested an iteration of the operation of the RyR array with constant coupling between neighboring RyRs, regardless of their functional state. Under such control conditions ( $e = 0.45$ ,  $\alpha = 1.0$ ), the high response and SNR were appropriately achieved, but the array opening lasted more than 70 ms (Fig. 5 A (a)). Then, it was found that the average opening duration under this condition was  $\sim 50$  ms, obviously longer than the physiologically expected 22 ms. Here, the question arose: how could a coupled system with high gain and optimal SNR be manipulated to realize fast termination?

The decoupling of activated RyRs provided an easy and efficient way. The decrease of “ $\alpha$ ” in our model resulted in the rapid closure of RyR array. As shown in Fig. 5 B, the decrease of “ $\alpha$ ” from 1.0 to 0.8 reduced the opening duration of RyR array from 50 ms to  $\sim 30$  ms (Fig. 5 A (b)). Further decrease “ $\alpha$ ” to 0.5 could shorten the duration of RyR array more to 15 ms (Fig. 5 A (c)).

To systematically investigate the effects of the decoupling of activated RyRs on the array’s duration of opening, we analyzed the termination behavior of RyR array under

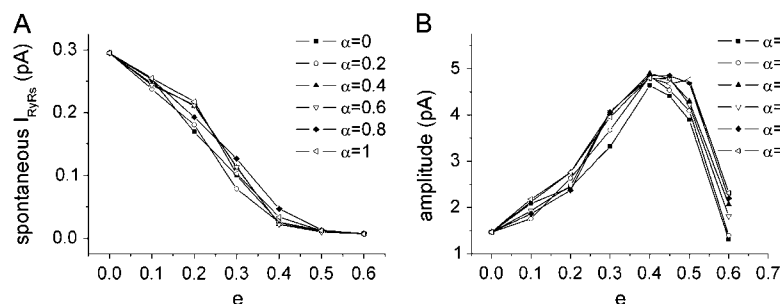


FIGURE 4 The  $e$ -dependent curves of system resting stability and response amplitude under various “ $\alpha$ ”. (A) The effect of “ $\alpha$ ” on the resting stability of RyR array. (B) The effect of “ $\alpha$ ” on the response amplitude of RyR array.

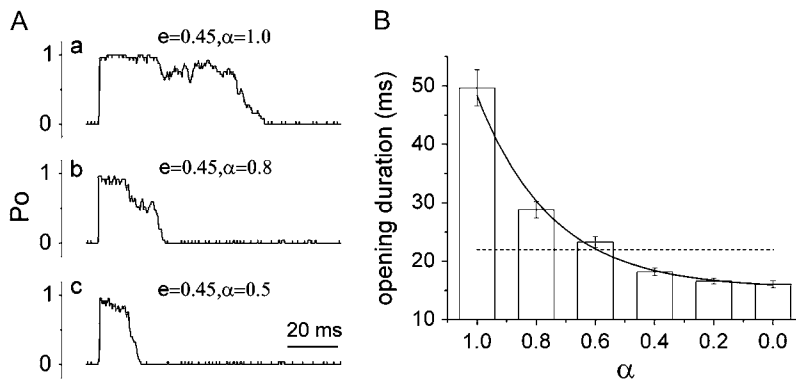


FIGURE 5 The effects of “ $\alpha$ ” on the opening duration of RyR array. (Aa) Array operation under control condition ( $e = 0.45, \alpha = 1.0$ ). (Ab) Array opening duration when “ $\alpha$ ” is reduced ( $e = 0.45, \alpha = 0.8$ ). (Ac) Array opening duration when “ $\alpha$ ” is further reduced ( $e = 0.45, \alpha = 0.5$ ). (B) The mean opening duration of RyR array could be modulated through adjusting the values of “ $\alpha$ ”, and the “ $\alpha$ ”-dependent curve could be well fitted to the exponential function (solid curve). The dashed line represents the expectation value of array opening duration (22 ms) according to the analysis of  $\text{Ca}^{2+}$  sparks and  $\text{Ca}^{2+}$  blinks.

different “ $\alpha$ ” (Fig. 5 B). When  $e$  was 0.45, we showed that the decrease of “ $\alpha$ ” induced an obvious reduction of opening duration. When “ $\alpha$ ” was set from 1 to 0 with the interval of 0.2, the opening duration of RyR array decreased quickly (Fig. 5 B), and the histogram could be well fitted with an exponential decay curve (Fig. 5 B, solid line). We noted that the system could be closed timely ( $\sim 20$  ms, indicated by dashed line in Fig. 5 B) when “ $\alpha$ ” was around 0.6. Compared with the coupling strength between resting RyRs ( $1.0 \times e$ ), the decreased coupling strength between activated RyRs ( $0.6 \times e$ ) is essential for RyR array to coachieve the rapid termination during  $\text{Ca}^{2+}$  release processes.

From the theoretical viewpoint, strong coupling between opening RyRs would delay the termination process by building high energy barrier to prevent the transition of RyRs from open state to closed state. The decoupling of activated RyRs would facilitate the rapid closure of RyR array. In addition, it should be clarified that “the decoupling of activated RyRs” itself is not a mechanism to trigger the termination process. The role of this regulatory mechanism within RyR array is to make the inherent termination mechanism (e.g.,  $\text{Ca}^{2+}$  inactivation, local SR depletion, etc.) work more efficiently.

#### A whole picture of “dynamic coupling” mechanism

We have shown that the optimal signal/noise ratio of RyR array can be achieved by suitable inter-RyRs coupling between resting RyRs and their neighbors, while decoupling of activated RyRs could facilitate the rapid termination of the system. The operation of the RyR array under one typical “optimal” condition ( $e = 0.45, \alpha = 0.6$ ) was simulated and shown in Fig. 6. This coupled system kept highly stable under rest and responded efficiently to the input  $\text{Ca}^{2+}$  signal, namely acquiring high SNR. Meanwhile, the mean array opening duration of RyR array was  $\sim 22$  ms and the decay constant of SR  $\text{Ca}^{2+}$  flux of  $\sim 5$  ms, which seemed to approximate the experimental and numerical estimation value in the work of Soeller and Cannell and Brochet et al. (19,22). Therefore, resting stability, high response efficiency, and fast

termination could be all satisfied through suitable regulation of inter-RyRs coupling, which could not be realized in either a completely uncoupled or a continued coupled system.

In an uncoupled system, the behavior of the array is completely controlled by  $\text{Ca}^{2+}$ . In this case, system gain cannot be enhanced without amplifying the array’s resting noise. For a completely coupled system, although both resting stability and high gain can be acquired, the continued coupling between activated RyRs exponentially prolongs the duration of system response. Loosening the coupling between activated RyRs would make opening RyRs behave more independently, benefiting the efficiency of negative feedback to close the system. Temporally asymmetric regulation of coupling, therefore, can control the system decay rate in the termination of  $\text{Ca}^{2+}$  release, while simultaneously maintaining an optimal SNR in the system response to the input  $\text{Ca}^{2+}$  signal.

Generally speaking, it is believed that the final goal of the biological system’s evolution is to optimize the system performance in its working environment. Our simulation predicts that the coupling between arrayed RyRs only occurs when necessary, the extent of which is finely controlled to satisfy

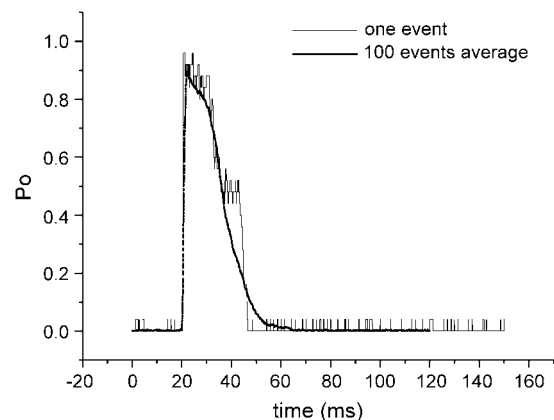


FIGURE 6 The simulating opening course of RyR array under representative optimal conditions ( $e = 0.45, \alpha = 0.6$ ). Thin solid curve is one simulation. Thick solid curve is the average of 100 simulations.

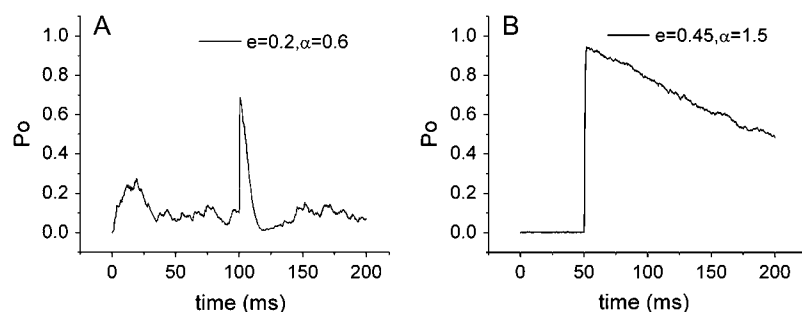


FIGURE 7 Biased coupling causes abnormal opening of RyR array. (A) Abnormality I: inter-RyR coupling is reduced. The baseline of array's activity under rest is high, but the system gain is low. (B) Abnormality II: the interaction between activated RyRs is enhanced, rather than reduced. Once the system is activated, it will be quite difficult to recover the static state (mean opening duration > 100 ms).

physiological requirements. Within the limitations of our system calculations, suitable coupling between RyRs ensures system stability, gain and SNR, while timely and partial decoupling of activated RyRs maintains the temporal order required of physiologically relevant system activity.

#### *Biased coupling between RyRs and abnormal SR $\text{Ca}^{2+}$ release*

Our calculations demonstrate that the extent of coupling strength always had an optimal value either in the initiation or the termination process of SR  $\text{Ca}^{2+}$  release. This implies that coupling is a significant regulatory point in SR  $\text{Ca}^{2+}$  signaling. By extension, it also suggests the potential relationship between biased inter-RyRs coupling and abnormal SR  $\text{Ca}^{2+}$  release.

For example, when the coupling between resting RyRs was weakened to a great extent ( $e = 0.2$ ,  $\alpha = 0.6$ ), the signal response curve exhibited high baseline and low response efficiency (Fig. 7 A). Loose coupling between resting RyRs would destabilize RyRs. Frequent spontaneous  $\text{Ca}^{2+}$  release from the leaky channels would potentially lead to the rise of resting  $\text{Ca}^{2+}$  in cytoplasm. Meanwhile, weakly coupled RyRs were also incapable of achieving the full activation of system, and only responded faintly to triggering  $\text{Ca}^{2+}$ . Totally, the system SNR in this situation becomes sufficiently low, which could result in low efficiency in SR  $\text{Ca}^{2+}$  handling.

A second scenario occurs when the coupling between activated RyRs was not decreased, but even increased. As shown in Fig. 7 B ( $e = 0.45$ ,  $\alpha = 1.5$ ), once the system is activated, it will be quite difficult to recover to static state. The mean opening duration of RyR array in this situation was longer than 100 ms, much longer than that acceptable in vivo. In principle, such prolonged opening of RyRs might be related to delayed termination of SR  $\text{Ca}^{2+}$  release events ( $\text{Ca}^{2+}$  spark, wave or transient), which might induce severe dysfunction of local or global SR  $\text{Ca}^{2+}$  handling system.

Here, we showed the potential relevance of biased inter-RyRs coupling, defined in our model, to the abnormal SR  $\text{Ca}^{2+}$  release. Because the  $\text{Ca}^{2+}$  release from SR is so important in muscle E-C coupling, the biased regulation of inter-RyR coupling might also be potentially involved in the dysfunction of muscle cells, especially in the pathological states.

#### *Compared with “conformational spread” model*

Another paradigm of interreceptor coupling exists in the two-dimensional array of bacterial chemotactic receptors (26). The model of “conformational spread” is proposed by Bray et al. to describe the cooperative behavior of chemotactic receptors (27). It was known that “conformational spread” conferred the chemotactic receptor array with several remarkable qualities, for instance, its ultrasensitivity, broad response spectrum ( $\sim 5$  orders of magnitude chemosensing capability), etc. (27–29).

It should be noted that the modulation of interreceptor coupling is the communal characteristic of “conformational spread” model and our “dynamic coupling” model. In “conformational spread” model, the interreceptor coupling should be modulated at different concentration of chemoattractants to harmonize the apparently antithetical requirements for both high sensitivity and a broad response spectrum (29). In our “dynamic coupling” model, the coupling strength is modulated at different channel functional states to coachieve the optimal signal/noise ratio and fast termination of  $\text{Ca}^{2+}$  release. Obviously, the modulation of interreceptor coupling could endow the 2-D receptor array with improved performance in cellular signal transduction.

## CONCLUSION REMARKS

We have proposed a novel design principle, temporally asymmetric coupling between neighboring RyRs, for RyR array to achieve the physiologically relevant resting stability and fast termination, which cannot be simultaneously acquired by either a completely uncoupled system or completely coupled system. Obviously, this is a simple and efficient way for RyR array to improve the signaling performance. Because the clustering of functional molecules commonly exists in biological systems, such design principle may be favored by other clustered receptors to achieve both rapid “on” and “off” response.

We thank Professor Pei-Hong Zhu, Hai-Ping Fang, Mu-Ming Zhang, Jianjie Ma, and Heping (peace) Cheng for fruitful discussion, and Dr. Jerome Parness for the modification of our manuscript.

This work was supported by a grant from the National Nature Science Foundation of China (NSFC30670495).



## REFERENCES

1. Rios, E., and G. Pizarro. 1991. Voltage sensor of excitation-contraction coupling in skeletal muscle. *Physiol. Rev.* 71:849–908.
2. Meissner, G. 1994. Ryanodine receptor/ $\text{Ca}^{2+}$  release channels and their regulation by endogenous effectors. *Annu. Rev. Physiol.* 56:485–508.
3. Bers, D. M. 2002. Cardiac excitation-contraction coupling. *Nature.* 415:198–205.
4. Fill, M., and J. A. Copello. 2002. Ryanodine receptor calcium release channels. *Physiol. Rev.* 82:893–922.
5. Soeller, C., and M. B. Cannell. 2004. Analysing cardiac excitation-contraction coupling with mathematical models of local control. *Prog. Biophys. Mol. Biol.* 85:141–162.
6. Stern, M. D., L. S. Song, H. Cheng, J. S. Sham, H. T. Yang, K. R. Boheler, and E. Rios. 1999. Local control models of cardiac excitation-contraction coupling. A possible role for allosteric interactions between ryanodine receptors. *J. Gen. Physiol.* 113:469–489.
7. Stern, M. D. 1992. Theory of excitation-contraction coupling in cardiac muscle. *Biophys. J.* 63:497–517.
8. Franzini-Armstrong, C., F. Protasi, and V. Ramesh. 1999. Shape, size, and distribution of  $\text{Ca}^{2+}$  release units and couplons in skeletal and cardiac muscles. *Biophys. J.* 77:1528–1539.
9. Yin, C. C., and F. A. Lai. 2000. Intrinsic lattice formation by the ryanodine receptor calcium-release channel. *Nat. Cell Biol.* 2:669–671.
10. Takekura, H., and C. Franzini-Armstrong. 2002. The structure of  $\text{Ca}^{2+}$  release units in arthropod body muscle indicates an indirect mechanism for excitation-contraction coupling. *Biophys. J.* 83:2742–2753.
11. Loesser, K. E., L. Castellani, and C. Franzini-Armstrong. 1992. Dispositions of junctional feet in muscles of invertebrates. *J. Muscle Res. Cell Motil.* 13:161–173.
12. Marx, S. O., J. Gaburjakova, M. Gaburjakova, C. Henrikson, K. Ondrias, and A. R. Marks. 2001. Coupled gating between cardiac calcium release channels (ryanodine receptors). *Circ. Res.* 88:1151–1158.
13. Bers, D. M., and M. Fill. 1998. Coordinated feet and the dance of ryanodine receptors. *Science.* 281:790–791.
14. Marx, S. O., K. Ondrias, and A. R. Marks. 1998. Coupled gating between individual skeletal muscle  $\text{Ca}^{2+}$  release channels (ryanodine receptors). *Science.* 281:818–821.
15. Stern, M. D., and H. Cheng. 2004. Putting out the fire: what terminates calcium-induced calcium release in cardiac muscle? *Cell Calcium.* 35: 591–601.
16. Sobie, E. A., K. W. Dilly, J. dos Santos Cruz, W. J. Lederer, and M. S. Jafri. 2002. Termination of cardiac  $\text{Ca}^{2+}$  sparks: an investigative mathematical model of calcium-induced calcium release. *Biophys. J.* 83:59–78.
17. Hu, X., X. Liang, K. Chen, H. Xie, Y. Xu, P. Zhu, and J. Hu. 2005. Modulation of the oligomerization of isolated ryanodine receptors by their functional states. *Biophys. J.* 89:1692–1699.
18. Dulhunty, A. F., P. Pouliquin, M. Coggan, P. W. Gage, and P. G. Board. 2005. A recently identified member of the glutathione transferase structural family modifies cardiac RyR2 substate activity, coupled gating and activation by  $\text{Ca}^{2+}$  and ATP. *Biochem. J.* 390:333–343.
19. Brochet, D. X., D. Yang, A. Di Maio, W. J. Lederer, C. Franzini-Armstrong, and H. Cheng. 2005.  $\text{Ca}^{2+}$  blinks: rapid nanoscopic store calcium signaling. *Proc. Natl. Acad. Sci. USA.* 102:3099–3104.
20. Xu, L., and G. Meissner. 2004. Mechanism of calmodulin inhibition of cardiac sarcoplasmic reticulum  $\text{Ca}^{2+}$  release channel (ryanodine receptor). *Biophys. J.* 86:797–804.
21. Bers, D. M., and V. M. Stiffel. 1993. Ratio of ryanodine to dihydropyridine receptors in cardiac and skeletal muscle and implications for E-C coupling. *Am. J. Physiol.* 264:C1587–C1593.
22. Soeller, C., and M. B. Cannell. 2002. Estimation of the sarcoplasmic reticulum  $\text{Ca}^{2+}$  release flux underlying  $\text{Ca}^{2+}$  sparks. *Biophys. J.* 82: 2396–2414.
23. Lukyanenko, V., I. Gyorke, S. Subramanian, A. Smirnov, T. F. Wiesner, and S. Gyorke. 2000. Inhibition of  $\text{Ca}^{2+}$  sparks by ruthenium red in permeabilized rat ventricular myocytes. *Biophys. J.* 79:1273–1284.
24. Bridge, J. H., P. R. Ershler, and M. B. Cannell. 1999. Properties of  $\text{Ca}^{2+}$  sparks evoked by action potentials in mouse ventricular myocytes. *J. Physiol.* 518:469–478.
25. Shimizu, T. S., S. V. Aksenov, and D. Bray. 2003. A spatially extended stochastic model of the bacterial chemotaxis signalling pathway. *J. Mol. Biol.* 329:291–309.
26. Maddock, J. R., and L. Shapiro. 1993. Polar location of the chemoreceptor complex in the *Escherichia coli* cell. *Science.* 259:1717–1723.
27. Duke, T. A., and D. Bray. 1999. Heightened sensitivity of a lattice of membrane receptors. *Proc. Natl. Acad. Sci. USA.* 96:10104–10108.
28. Bray, D., and T. Duke. 2004. Conformational spread: the propagation of allosteric states in large multiprotein complexes. *Annu. Rev. Biophys. Biomol. Struct.* 33:53–73.
29. Bray, D., M. D. Levin, and C. J. Morton-Firth. 1998. Receptor clustering as a cellular mechanism to control sensitivity. *Nature.* 393:85–88.